THE PENNSYLVANIA STATE UNIVERSITY
SCHREYER HONORS COLLEGE

DEPARTMENT OF ENGINEERING SCIENCE AND MECHANICS

A MECHANICAL MODEL OF A HUMAN ARM MAKING A SHOT ON GOAL IN AIR HOCKEY: ERROR SENSITIVITY AND GOAL EQUIVALENCE

ZACHARY MORGEN
SPRING 2022

A thesis
submitted in partial fulfillment
of the requirements
for a baccalaureate degree
in Engineering Science
with honors in Engineering Science

Reviewed and approved* by the following:

Dr. Joseph Cusumano
Professor of Engineering Science and Mechanics
Thesis Supervisor

Dr. Christian Peco
Assistant Professor of Engineering Science and Mechanics
Honors Adviser

Dr. Judith Todd
Department Head
P.B. Breneman Chair and Professor of Engineering Science and Mechanics

* Electronic approvals are on file.

ABSTRACT - Technical

A big question in the field of neuroscience concerns brain lateralization and the motion controls that each hemisphere of the brain implements. The dynamic dominance model states the left hemisphere (in right handers) is proficient at predictive control, while the right hemisphere is proficient at impedance control [1]. Predictive control schemes output precisely timed and synchronized muscle forces to needed to accomplish a goal-directed task, whereas impedance control schemes adjust the effective stiffness and damping properties of the limbs to reject unexpected disturbances. To investigate this claim, a mechanical model of a human arm taking a shot in air hockey was constructed. The two-link model is impedance-based in that its joint torques are generated by effective stiffness and damping properties modeled using torsional springs and dampers. The equations of motion for the arm mechanism and for the puck after it is struck. The game of air hockey provides an example of a goal-directed task. Simulations of our model were used to study how its accuracy depends on system parameters. This is done by first finding the goal function for the task, which is then used in to determine a *goal equivalent manifold* (GEM) for the arm as it executes a single shot on goal. The GEM maps system parameters (e.g., stiffnesses and damping coefficients) to error at the goal. The GEM provides a fundamental way to quantify and visualize the sensitivity of the task performance (i.e., error at the targe) to changes in system parameters. This geometric characterization of sensitivity allows us to simulate the relation between fluctuations in body-level variability and goal variability at the target position of the air hockey game. This was done by examining fluctuations in impedance elements, and how further deviations in those values result in a larger goal-level error at the target. Specifically, deviations in system parameters that are normal to the tangent plane of the GEM.

ABSTRACT – Non-Technical

Previous research has shown that the left and right hemispheres of the brain control the contralateral portions of the body. While this fact is well established, the control schemes used by each hemisphere to control movement is not yet understood. The Dynamic Dominance Model sheds some light on this question by positing that the left hemisphere (in right handers) employs a predictive control scheme while the right hemisphere employs an impedance motion control scheme. The main difference between the two schemes is that predictive control schemes output synchronized muscle forces to accomplish some goal-directed movement task, whereas impedance control adjusts effective stiffness and damping properties of the limbs when stabilization and disturbance rejection is of paramount importance. To test the different control schemes, a mathematical model of a human playing air hockey was created. This model consists of a two-link mechanism that mimics the upper arm and forearm. Also included in the model is the collision between the free end of the arm and the puck, and the subsequent sliding motion of the puck until it comes to a stop. The mathematical model developed here focuses on impedance control by modeling the joint torques as torsional springs and dampers. Sensitivity analysis was performed to show how variability in system parameters is related to error at the target for shots in an air hockey game.

TABLE OF CONTENTS

LIST OF FIGURES

LIST OF TABLES

ACKNOWLEDGEMENTS

First and foremost, I would like to thank my advisor, Dr. Cusumano, for his continuous support and guidance throughout this project. He has pushed me to become the best possible engineer I can be by not only trusting me, but also holding me to high expectations. Dr. Cusumano has taught me many lessons that I know has made me a better engineer and person, and I will carry those lessons with me into graduate school and in life. Finally, I would like to thank my family for their support all throughout my college career.

Chapter 1

Introduction

An important question in biology is how brain lateralization contributes to the control of human movement. People have long accepted that the brain is divided into a left and right hemisphere. However, many still wonder about the motion control schemes that each hemisphere implements. In other words, people want to investigate how handedness flows from brain lateralization and its impact on the motor control processes used by each hand. One hypothesis on the nature of handedness in human motor control is the dynamic dominance model (DDM) [1]. In this model, the left hemisphere (in right handers) utilizes predictive motion control, while the right hemisphere employs an impedance control process [1]. A predictive control process is used for precise goal-directed movements such as, throwing a ball to hit a desired target. An impedance control system consists of adjustable springs and dampers or, more generally, elastic and viscoelastic elements. The DDM posits that impedance control processes are used to minimize potential errors when unexpected mechanical conditions are met. For example, when someone slices meat, the non-dominant hand uses the fork to stabilize the meat via impedance control, while the dominant hand holds the knife and cuts it using predictive control [2]. Impedance control adjusts the effective stiffness and damping properties of the limbs, whereas predictive control outputs timed synchronized forces needed to accomplish some task.

The focus of this thesis is on impedance control. To do this, the game of air hockey was chosen, specifically the task of taking a shot on goal. The game of air hockey is modeled by using a planar mechanism with 2 degrees of freedom (DOF) that provides a simplified representation of a human arm. Consistent with the aim of studying impedance control, torsional springs and

dampers will be used to represent the effective viscoelastic properties of muscles providing torques at each of the model's two joints. In a previous study [3], researchers performed an experimental study of humans playing game of shuffleboard and examined the fluctuations of the errors at the target over hundreds of shots. Using the results of their experiments, the researchers showed how body level noise scales with intrinsic body-level noise via the total *body-goal sensitivity*. This was a result of observing fluctuations in task performance at both the body and goal levels and performing statistical correlations to relate task variability to goal variability. [3].

Air hockey and shuffleboard are examples of goal directed tasks, in which the goal is for the puck to stop at a target point. Such a well-defined task will lead to a goal function, which serves as a hypothesis for the strategy being used to execute the task [3] and takes as its arguments system parameters. The zeros of the goal function correspond to system parameters that result in perfect task execution. In our model, the goal function take as arguments the stiffness and damping coefficients, as well as other parameters related to the joint viscoelastic properties, . In this case, the zeros of the goal function correspond to a shot for which the puck stops exactly at the target point. Nonzero values of the goal function correspond to the task error, which in this case is simply the distance of the stopped puck from the target. The goal function can also be used to create the *goal equivalent manifold* (GEM), which is a surface in the system's parameters space that contains all possible combinations of the system parameters that give perfect task execution [3,4,6]. The GEM also provides insight to the sensitivity of the task to parameter errors: parameter variations perpendicular to the GEM result in task errors, whereas errors tangent to the GEM result in zero error. Sensitivity analysis allows us to quantify the degree to which "body-level" (i.e., system) parameter errors are amplified at the goal level and, in combination with the GEM, provides a geometrical interpretation of how error is generated.

Our model consists of two links with one pinned end and one free end, so that the 2 DOF arm model is mechanically equivalent to a double pendulum moving in the horizontal plane. The

pinned end of the model corresponds to the human shoulder, and the free end corresponds to the hand or “end effector” holding the air hockey mallet that is used to strike the puck. To actuate the mechanism, torsional springs and dampers are placed at the pinned joint (the shoulder) and the hinge joint between the two links (the elbow). These viscoelastic elements can be adjusted as part of the impedance control scheme. The other component of the air hockey game is a puck, which is put into motion by a collision between it and the mallet. The collision will be modeled using standard oblique impact mechanics, and the subsequent sliding motion of the puck will be modeled assuming Coulomb friction.

This thesis presents the construction of the complete model, including the dynamics of the arm for arbitrary joint torques, the collision with the puck, and the puck’s subsequent motion. Thus, the model will require determination of the equations of motion for the two-link mechanism and analysis of the oblique impact between the mechanism and the puck. Numerical experiments for the model arm performing repeated shots on goal will be carried out. The numerical experiments will be used to test the effect of different parameters on the motion of the mechanism and the accuracy of the puck’s final resting position. This will lead to the mathematical analysis of sensitivity of shots on goal to small deviations in the parameters which, in turn, will be used to obtain the GEM for the system.

The results from this thesis will begin to answer the questions about brain lateralization and how motion control schemes are a direct consequence of that. The work presented in this study focuses on how variability in effective joint stiffnesses and damping relates to goal variability. This research has the potential to aid in the diagnosis and rehabilitation of neurological injuries. Health care providers that care for people with neuromotor disorders (e.g., Parkinsonism) would know what neuromotor process is failing and they would be able to receive a personalized treatment plan by observing how fluctuations errors observed during repeated performance at the body level are mapped to goal level errors. While this study has focused on

the effect of system impedances (i.e., stiffnesses and damping), the model can be adapted to incorporate arbitrary joint torques appropriate for predictive control simulations. It is hoped that the model will therefore be useful for others interested in examining questions about brain lateralization and its effect on motor control in humans.

Chapter 2

Literature Review

2.1: Brain Lateralization and Motor Control

Previous studies that investigate brain lateralization have shown that each hemisphere of the brain is responsible for a different motion control process [1]. When coupled together, these motion control processes perform tasks. To investigate these motion control processes, Sainburg and his colleagues have developed a model of motor lateralization [1]. There focus is the dynamic dominance model, which states that, that the left hemisphere (in right handers) is specialized for predictive control, and the right hemisphere is specialized impedance control for the stabilization of motion [1]. The predictive control assures both mechanical and trajectory efficiency under stable conditions, while impedance control accounts for the robustness when motion is faced with unpredictable conditions [1]. The model presented in this thesis was created with impedance control in mind. Mechanical impedance has an effective stiffness and damping value or, more generally, elastic and viscoelastic elements. A mechanical impedance can be modeled by using a torsional spring as a motion actuator. The air hockey model consists of torsional springs placed at the shoulder and elbow joints respectively to actuate the motion.

There was an experiment done in which participants played a virtual shuffleboard game. This game involved participants playing a virtual game of shuffleboard with the goal to slide the puck a certain distance [3]. The air hockey model will have the same goal of having the puck travel a certain distance. Will an explicit goal defined, the error for each trial was computed. This was done by comparing the final position of the puck to the desired final position of the puck [3]. The analysis of this error is what gives rise to answering questions about motion control schemes

in a person's dominant and non-dominant hand. The focus of this research is to create the model, with the idea that others may use it to gather data about motion control schemes.

Another experiment that was conducted to examine brain lateralization and motion control involved a targeting-reaching task using both their dominant and non-dominant hand [4]. In this task, participants were asked to place their index finger at a certain starting point and orientation, then they had to reach for a target in both medial and lateral directions [4]. The medial direction is the direction in which the medial target and the length of the index finger are colinear [4]. The lateral direction is the direction that is orthogonal to the medial direction. The results of these experiments were angular kinematic data for the position of hand, and the location of the hand as time progressed. These sets of data were then differentiated to yield velocity values. From these results, the researchers were able to show that on trials where the participant was asked to move laterally, the dominant arm movements were consistent with motion control that predictively accounts for associated changes in arm mechanics [4]. They were also able to show, for these orthogonal tasks, that the non-dominant arm movement was an equilibrium point control strategy [4]. This led to their conclusion that separate motion control schemes could in fact coexist in different regions of the brain.

The model of a human playing air hockey takes elements from both experiments. There is a reaching task and the collision with a puck. As in [4], the mechanism for the human arm must reach to contact the puck. Furthermore, the mechanism must reach such that it strikes the puck with sufficient energy to ensure that the puck stops on the target point. The combination of design elements from these experiments gives a straightforward way for analyzing the game of air hockey.

2.3: Goal Functions and Goal Equivalent Manifolds

The shuffleboard experiment included an analysis technique that is based on a sensitivity analysis technique that is based on the goal equivalent manifold (GEM) concept. The GEM technique differs from other analysis techniques because this technique makes direct use of a goal function [3]. Manifolds are surfaces that exist in a suitably defined space of state variables [3]. Goal functions provide theoretical definitions of the sensitivity that is independent of any applied motion [3]. The zeros of the goal function correspond to zero error, or a task being executed perfectly. For the shuffleboard game, the goal function was determined by finding an equation of motion (EOM) for the puck using Newtonian mechanics and combing that with the goal-error equation. The goal error equation provides the error for each trial and is determined by comparing the puck's final position to the desired final position [3]. A similar process will be used to determine the goal function for the air hockey model. Newtonian mechanics will be applied to determine EOMs for both the arm mechanism, and the collision between the arm and the puck. These equations when combined with the same error equation from the shuffleboard game, will give the goal function and the GEM.

The goal equivalent manifold concept was initially developed in 2006 to study the relationship between variability at the body and goal levels using sensitivity analysis [5]. In [5], the authors derive a general formula that expresses the relationship between goal-level errors to body-level perturbations. The general formula that the authors developed was the goal function. The general formula means that GEM analysis can be applied to not just a reaching task, like shuffleboard and air hockey, but any motor control in which a clear goal is defined. For example, in [6], the researchers state that GEM is applicable to walking tasks and throwing tasks in addition to reaching [6]. The goal function for those walking on the treadmill revealed the participants must, over time, walk at the same average speed of the treadmill and stay at the same

average position [6]. Another example involved a throwing ball with the goal of having to hit a target a certain distance and height away [6]. The researchers used elementary projectile motion mechanics to determine the goal function. In both examples, the researchers went to show the relationship between body variability and goal variability by analyzing how fluctuations in the body (system parameters) affected goal-level error.

The space that makes up the GEM are relevant state variables for the model. The way of determining a portion of the GEM involves linearization the goal function. This results in the tangent plane on a portion of the GEM at a set of system parameters that result in an error of zero, or the task being executed perfectly [7]. Since the air hockey model will be using torsional springs as motion actuators, the stiffnesses and damping coefficients will be included in this task variable space. The advantage of GEM analysis is that this analysis can be used to find other combinations of system parameters that also yield perfect task execution. For this, a known set of system parameters that result in perfect task execution is needed. Once this set of parameters is obtained, the manifold that "sweeps" out additional solutions is determined from the Jacobian matrix for the goal function because all points that lie on the tangent plane to the GEM will result in perfect task execution [7]. Also contained within this Jacobian, are sensitivity values for how the system responds to small perturbations in each state variable [7]. This is important for not only understanding how the model works, but also for answering the question about the different brain hemispheres and the control scheme each implement. This is done by examining the singular value decomposition (SVD) of the Jacobian [7]. For a goal directed motion, the SVD reveals that fluctuations in system parameters that are orthogonal to the tangent plane result in the greatest goal-level error. In other words, normal deviations in system parameters result in higher variability at the target. To investigate these deviations, empirical probability distributions of a set of system parameters are used to show how fluctuations map to goal-level error at the target.

2.4: Conclusion

The motion control schemes implemented by the left and right hemispheres has been questioned by many. The Dynamic Dominance Model suggests that the left hemisphere (in right handers) is for predictive motion control, and the right hemisphere is for impedance control. There have been several experiments that used goal directed motion to examine brain lateralization. One such experiment asked participants to reach with their hand, and the results showed that movements by dominant arm reflected predictive motion, while the non-dominant arm reflected impedance control [4]. Another experiment that was done using a shuffleboard game. This game had the goal of sliding a puck a certain distance. To examine the results, the researchers performed GEM analysis and were able to show how the normal and tangent surfaces to the GEM reflected different motion control schemes [3]. The air hockey model will involve finding the tangent surface to the GEM at a set of system parameters and analyzing how slight fluctuations in those parameters affect goal-level error.

Chapter 3

Design of the Model

The model consists of two major elements. The first is a two-link mechanism that models the arm, and the second is a collision between the two mechanism and puck. The work presented in this chapter goes through the derivation of the equations of motion for both elements, and a stability analysis for the two-link mechanism.

3.1: Two-Link Mechanism for Human Arm

The motion for the arm of a human playing air hockey is represented by an open-loop two-linked mechanism as shown in **Figure 1** (left); where, links 1 and 2 represent the humerus and forearm, respectively. Therefore, points *O* and *A* represent the glenohumeral joint (shoulder) and synovial joint (elbow), respectively. The free body diagrams (FBDs) of the two-link mechanism are also shown in **Figure 1** (right). The FBDs show the reaction forces at points O and A respectively. Moments M_O and M_A are applied moments that can be changed to test the different motion control schemes.

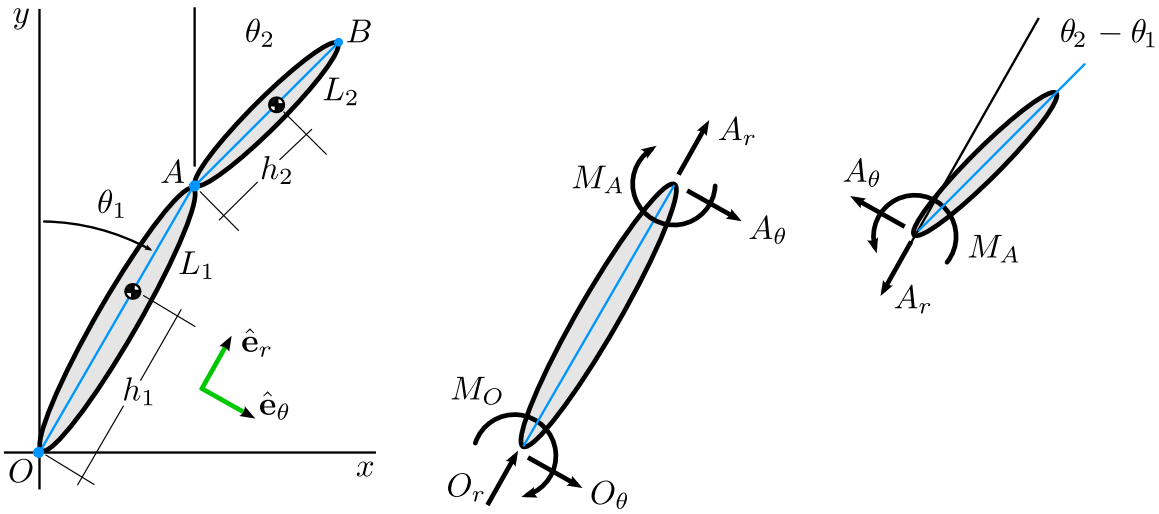

Figure 1. Schematic for two-link mechanism: (left) polar basis and link coordinates; (right) free body diagrams. The joint moments $\boldsymbol{M_O}$ and $\boldsymbol{M_A}$ can be varied to for different applications. In this work, the moments are provided by "impedance" elements (i.e., torsional springs and dampers).

The Newton-Euler equations, eq (1), require that the coordinate basis be relative to a fixed point. The cylindrical-polar basis will therefore be relative to fixed point *O*, where $\widehat{\mathbf{e}_\mathbf{r}}$ is colinear with points *O* and *A*, $\widehat{\mathbf{e}_\boldsymbol{\theta}}$ is directed 90 degrees clockwise, and $\widehat{\mathbf{e}_\mathbf{r}} \times \widehat{\mathbf{e}_\boldsymbol{\theta}} = \hat{\mathbf{k}}$.

$$\begin{aligned} \mathbf{F} &= m\ddot{\mathbf{r}}_\mathbf{G} \\ \mathbf{M} &= I_G\boldsymbol{\alpha} \end{aligned} \tag{1}$$

The angular velocity of the cylindrical-polar basis is then.

$$\boldsymbol{\omega}_{\mathbf{r\theta k}} = \dot{\theta}_1\hat{\mathbf{k}} \tag{2}$$

The position vectors for the center of mass (COM) of each link.

$$\mathbf{r_1} = h_1\widehat{\mathbf{e}_\mathbf{r}} \tag{3}$$

$$\mathbf{r_2} = (L_1 + h_2\cos(\theta_2 - \theta_1))\widehat{\mathbf{e}_\mathbf{r}} + h_2\sin(\theta_2 - \theta_1)\,\widehat{\mathbf{e}_\boldsymbol{\theta}} \tag{4}$$

The acceleration of each link's center of mass is then.

$$\ddot{\mathbf{r}}_1 = -h_1\dot{\theta_1^2}\,\widehat{\mathbf{e_r}} + h_1\ddot{\theta}_1\,\widehat{\mathbf{e_\theta}} \tag{5}$$

$$\begin{aligned}\ddot{\mathbf{r}}_2 = &\left(-L_1\dot{\theta_1^2} - h_2\left(\cos(\theta_2-\theta_1)\,\dot{\theta_2^2} + \sin(\theta_2-\theta_1)\,\ddot{\theta}_2\right)\right)\widehat{\mathbf{e_r}} \\ &+ \left(L_1\ddot{\theta}_1 + h_2\left(-\sin(\theta_2-\theta_1)\,\dot{\theta_2^2} + \cos(\theta_2-\theta_1)\,\ddot{\theta}_2\right)\right)\widehat{\mathbf{e_\theta}}\end{aligned} \tag{6}$$

The total force on each link is:

$$\mathbf{F_1} = (O_r + A_r)\widehat{\mathbf{e_r}} + (O_\theta + A_\theta)\widehat{\mathbf{e_\theta}} \tag{7}$$

$$\mathbf{F_2} = -A_r\widehat{\mathbf{e_r}} - A_\theta\widehat{\mathbf{e_\theta}} \tag{8}$$

The moments on each link taken about each links COM is

$$\mathbf{M_1} = (M_o + M_A - h_1 O_\theta + A_\theta(L_1 - h_1))\hat{\mathbf{k}} \tag{9}$$

$$\mathbf{M_2} = (-M_A + A_\theta h_2\cos(\theta_2-\theta_1) - A_r h_2\sin(\theta_2-\theta_1))\hat{\mathbf{k}} \tag{10}$$

Assume that links 1 and link 2 are identical think bars ($h_1 = h_2 = \frac{L}{2}, m_A = m_O = m, I_1 = I_2 = \frac{1}{12}mL^2$) and apply the Newton-Euler equations, the EOMs for the two-link mechanism are:

$$Let, \Delta = \frac{1}{L^2 m(-23 + 9\cos(2(\theta_2-\theta_1)))}$$

$$\begin{aligned}\ddot{\theta}_1 = \Delta 3\Big(&8M_A + 8M_O + 12M_A\cos(\theta_2-\theta_1) + 3L^2 m\sin(2(\theta_2-\theta_1))\,\dot{\theta_1^2} \\ &+ 4L^2 m\sin(\theta_2-\theta_1)\,\dot{\theta_2^2}\Big)\end{aligned} \tag{11}$$

$$\begin{aligned}\ddot{\theta}_2 = \Delta\Big(&96M_A + 36M_A\cos(\theta_2-\theta_1) + 36M_O\cos(\theta_2-\theta_1) \\ &+ 48L^2 m\sin(\theta_2-\theta_1)\dot{\theta_1^2} + 9L^2 m\sin(2(\theta_2-\theta_1))\,\dot{\theta_2^2}\Big)\end{aligned} \tag{12}$$

In equations (11) and (12) applied moments M_A and M_O have no specific form. For an analysis on predictive control the applied moments will torque time series because the dynamic dominance model hypothesizes predictive control as muscle forces that are timed and synchronized to execute a task. As mentioned before, the focus of this thesis is an impedance-based model. The applied moments will take on the form of torsional springs shown in equations (13) and (14). In

these equations, κ represents an effective stiffness and c represents an effective damping. An effective stiffness and damping is necessary because muscles in the shoulder and elbow co-contract to vary the stiffness and damping needed for different tasks.

$$M_O = \kappa_O(\theta_1 - \theta_{O0}) + c_O\dot{\theta}_1 \tag{13}$$

$$M_A = \kappa_A(\theta_2 - \theta_1 - \theta_{A0}) + c_A(\dot{\theta}_2 - \dot{\theta}_1) \tag{14}$$

The EOMs now feature effective spring stiffness and damping coeffects that can be adjusted to change the motion of the mechanism. The unstretched spring angles are θ_{O0} and θ_{A0}. The unstretched spring values will provide a way of not only confirming the EOMs, but a way of determining where the mechanism will ultimately come to rest.

3.1.1: Stability Analysis

The equilibrium positions of the two-link mechanism were determined by substituting equations (13) and (14) into the equations of motion, (11) and (12), and setting $\ddot{\theta}_2 = \ddot{\theta}_1 = \dot{\theta}_2 = \dot{\theta}_1 = 0$ yields equations (15) and (16).

$$\theta_1^* = \theta_{O0} \tag{15}$$

$$\theta_2^* = \theta_{O0} + \theta_{A0} \tag{16}$$

The equilibrium positions of the spring are the unstretched torsional spring angles. These equilibrium expressions allow us to validate EOMs.

To simulate the EOMs with the torsional spring moments applied, values for the mass and length are needed. Take the mass of each link to be $m = 1\ kg$ and the length to be $L = 1\ m$. For this simulation, the puck is placed at $(x_P, y_P) = \left(0, \frac{3}{2}L\right)$. In order for the free end of the mechanism to damp out to this point, the angles the result in the position of point B resting on this point are needed. The position of point B (mallet) is represented by equation (17).

$$\mathbf{r_B} = x_B\hat{\mathbf{I}} + y_B\hat{\mathbf{J}} = L(\sin(\theta_1) + \sin(\theta_2))\hat{\mathbf{I}} + L(\cos(\theta_1) + \cos(\theta_2))\hat{\mathbf{J}} \quad (17)$$

Setting the puck position equal to the position of point, and solving the non-linear system of equations, equation (17), for θ_1 and θ_2 gives:

$$\theta_1 = 0.7227\ rad, \theta_2 = -0.7227\ rad$$

If these are to be the equilibrium angles, then equations (15) and (16) give the unstretched spring angles:

$$\theta_{O0} = 0.7227\ rad, \theta_{A0} = -1.4454\ rad$$

The two-link mechanism should now come to rest at $\theta_1 = 0.7227\ rad, \theta_2 = -0.7227\ rad$. The additional parameters and initial conditions needed for the simulation are shown in **Table 1**. These initial conditions represent the humerus and the forearm laying on x-axis crossed over each other.

Table 1. Table of Parameters Used in Stability Analysis

Initial Conditions	Value	Spring Parameter	Value
θ_{10}	$\frac{\pi}{2}$	κ_O	$10\ N\,m\,rad^{-1}$
$\dot{\theta}_{10}$	$0\ m/s$	c_O	$5\ J\,s\,rad^{-1}$
θ_{20}	$-\frac{\pi}{2}$	κ_A	$10\ N\,m\,rad^{-1}$
$\dot{\theta}_{20}$	$0\ m/s$	c_A	$5\ J\,s\,rad^{-1}$

Figure 2 is a plot of the angles after numerically integrating the equations of motion.

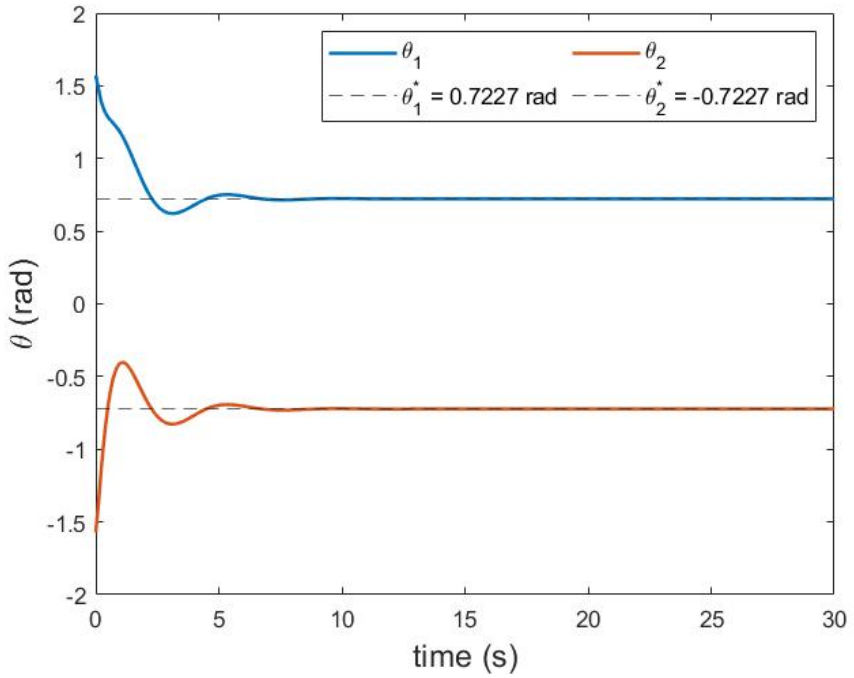

Figure 2. Equilibrium positions of two-link mechanism with impedance elements. This figure shows that the system does indeed damp out to the unstretched torsional spring angle at each joint, which are adjustable system parameters. The fact that the lines in the figure do not cross indicates that the humerus and the forearm do not cross over each other, as required for the mechanism to approximate the action of a human arm taking a shot in air hockey.

Angles θ_1 and θ_2 not only start at the correct initial conditions, but they also damp out to the angles that correspond to the puck position of $(x_P, y_P) = \left(0, \frac{3}{2}L\right)$. The choices for the effective spring dampness and damping were chosen to ensure that the motion of the mechanism mimic a human arm striking the puck with adequate force to move the puck. This is equivalent to a "follow through motion" where the objective to go through the motion. In this context, a person striking through the puck for more power.

3.1.2: Rotation Angle β

The equilibrium angles were chosen for the puck position of $\left(0, \frac{3}{2}L\right)$. However, the mechanism needs to strike the puck for any initial puck placement on the y-axis. This is done by first

determining the path of the free end for a given set of system parameters, and then calculating the distance from each point on that path to point *O*. This distance is then compared to the distance between the puck and point *O*. Once these two distances are equal, the angle β (measured clockwise from the positive y-axis) is calculated from the point on the path of *B* that achieved this distance. The simulation is then executed again after updating the parameters shown in equation (18). The re-execution of the simulation would be the equivalent of human playing air hockey, missing the puck, and adjusting the effective spring and damping values to ensure that the puck is struck on the next attempt.

$$\begin{aligned} \theta_{10} &\rightarrow \theta_{10} - \beta \\ \theta_{20} &\rightarrow \theta_{20} - \beta \\ \theta_{A0} &\rightarrow \theta_{A0} - \beta \end{aligned} \tag{18}$$

The plot on the left in **Figure 3** is the path of B that is not rotated by β, and the plot on the right shows the path of *B* after it has been rotated by beta. For this simulation, the puck has been placed at $(0, 1.2\ m)$. The system parameters are equivalent to the ones in **Table 1**.

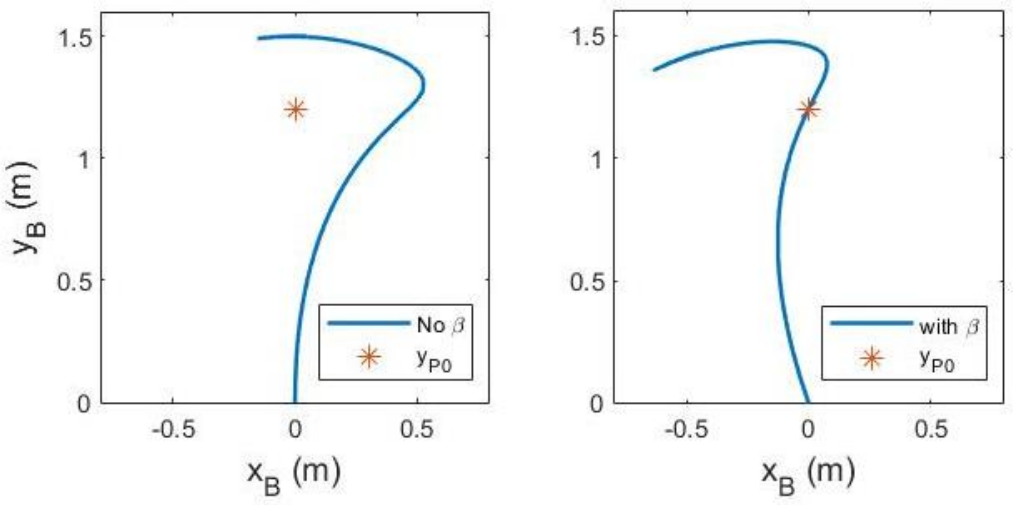

Figure 3. Obtaining an arm movement that strikes the puck. (left) Example path of mallet (i.e., the free end of the two-link arm) for typical initial condition: the mallet does not strike the puck located at y_{p0}. (right) Path of mallet rotated by the appropriately computed angle β. The rotation of the path ensures that the mallet not only strikes the puck but that the line of impact between the puck and the mallet is the *y*-axis. Restricting the line of impact to the *y*-axis was done to simplify the analysis for this preliminary study and corresponds to the case of a person launching the puck straight ahead.

3.2: Mallet and Puck Collision

The rotation angle β not only ensures that the mechanism will hit the puck, but it will strike the puck such that the line of the impact of the collision is collinear with the y-axis. This means the puck will travel only along the y-axis after the collision. The equation of the motion was determined by applying Newton's second law for a sliding object.

$$y = y_0 + V_0 t - \frac{1}{2}\mu_k g t^2 \tag{19}$$

The initial velocity of the puck (V_0) was determined by applying the impact law given by equation (20).

$$e = \frac{V_B^+ - V_P^+}{V_P^- - V_B^-} \tag{20}$$

Where, *e* is the coefficient of restitution and the " $+$ " and " $-$ " superscripts denote the velocity after and before the collision, respectively. When the player strikes the puck in air hockey, they follow through for increased accuracy and power. Therefore, V_B^- is approximately equal to V_B^+, $V_B^- \cong V_B^+$. This assumption substituted into the impact law along with the fact the puck starts at rest gives the initial velocity of the puck.

$$V_0 \triangleq V_P^+ = (1 + e)V_B^- \tag{21}$$

Now, all that is needed is the velocity of point B (free end), which is determined by taking the time derivative of equation (17).

$$\dot{\mathbf{r}}_\mathbf{B} = L\big(\cos(\theta_1)\dot{\theta}_1 + \cos(\theta_2)\dot{\theta}_2\big)\hat{\mathbf{I}} - L\big(\sin(\theta_1)\dot{\theta}_1 + \sin(\theta_2)\dot{\theta}_2\big)\hat{\mathbf{J}} \tag{22}$$

The numerical solutions of the EOMs, equations (11) and (12), for the two-link mechanism will provide the values needed to calculate the velocity of point B.

3.3: The Goal Function

To perform a shot, the model needs several parameters listed in **Table 2**.

Table 2. System Parameters and Task Variables for the Model

System Parameter	Description	Task Variable	Description
θ_{10}	Initial Position of θ_1	κ_O	Spring Stiffness at O
$\dot{\theta}_{10}$	Initial Velocity of θ_1	c_O	Spring Damping at O
θ_{20}	Initial Position of θ_2	θ_{O0}	Unstretched Spring Angle at O
$\dot{\theta}_{20}$	Initial Velocity of θ_2	κ_A	Spring Stiffness at A
μ_k	Kinetic Friction coefficient	c_A	Spring Damping at A
e	Coefficient of Restitution	θ_{A0}	Unstretched Spring Angle at A
		y_{P0}	Initial Puck Position

Since the focus of this model is on how changes in task variables affect motion, the system parameters will be consistent in every numerical experiment. With the system parameters fixed, the function that takes as its inputs the spring and the initial puck position variables and outputs the position where the puck comes to the rest. This function is the goal function for the air hockey game.

$$y_{Pf} = y = f(\kappa_O, c_O, \kappa_A, c_A, \theta_{O0}, \theta_{A0}, y_{P0}) = f(\mathbf{q}) \tag{23}$$

The goal-level error (e_y) for a target stopping point (x_T, y_T) is now determined by:

$$e_y = y - y_T = f(\mathbf{q}) - f(\mathbf{q}^\star) \tag{24}$$

where, $\mathbf{q}^\star$ is the vector that contains the task variables in which the puck stops at (x_T, y_T), to within some error. So, by definition, an error of zero means the **q** vector used for that shot, stopped exactly on the target point.

Chapter 4

GEM and Simulations

As an example, say that the goal is to have the puck to stop on the target point of $(x_T, y_T) = (0,7L)$. The task variables can all be adjusted to determine which set does indeed hit the target, to within a certain error. Since the model is impedance based, the focus will be examining how slight changes in spring stiffnesses and initial puck placement affect the final puck placement.

4.1: The Goal Equivalent Manifold (GEM)

The GEM is the result of a sensitivity analysis around a set of parameters that hit the target point (0,7L). So, before the GEM is constructed, a set of task variables that hit the target point needs to be determined. The numerical values that are contained within this vector are given in **Table 3**, and these values result in an error that is on the order of 10^{-4}.

Table 3. Task Variables that Result in 10-4 Error for the Target Position (0,7L) in SI Units

Task Variable	κ_O	c_O	κ_A	c_A	θ_{O0}	θ_{A0}	y_{P0}	y_{Pf}
Value	10	5	10	5	0.7227	-1.4454	0.4466	6.99672

Now that $\mathbf{q}^\star$ is known, the sensitivity analysis for the GEM can be constructed by performing the Taylor expansion of (24), which gives:

$$e_y = f(\mathbf{q}^\star) + \frac{\partial f}{\partial \mathbf{q}}(\mathbf{q}^\star)\Delta\mathbf{q} + O(h^2)$$
$$Where;\ \frac{\partial f}{\partial \mathbf{q}} \equiv \nabla f \tag{25}$$

Since $f(\mathbf{q}^\star) \cong 0$ and the fluctuations are small, higher order terms can be ignored. The geometric sensitivity of each task variable is now known. The lowest order error (linear term from Taylor expansion) is now.

$$e_y = (\nabla f)^T \Delta \mathbf{q} \tag{26}$$

There are an infinite number of values for **q** that give result in 0 error, corresponding to simulations where the puck stopped exactly on the target. The tangent plane to GEM is therefore the set of points in the task variable space:

$$T_G(\mathbf{q}^\star) = \{\Delta \mathbf{q} \mid \left(\nabla f(\mathbf{q}^\star)\right)^T \Delta \mathbf{q} = 0\} \tag{27}$$

This surface exists in 7D task variable space, where those dimensions correspond to the elements of **q**. Since the GEM is the set of points that result in zero error, equation (27) can also be expressed as.

$$\sum_{i=1}^{7} \frac{\partial f}{\partial \mathrm{q}_i}(\mathbf{q}^\star)(\Delta \mathrm{q_i}) = 0 \tag{28}$$

However, since the visualization of a surface in a 7D space is difficult, the focus will be on three task variables to vary and hold the rest constant. Substituting the 3 chosen task variables (spring stiffnesses and initial puck position) into equation (28), gives the equation for the tangent plane to GEM, shown in **Figure 1**.

$$\Delta y_{P0} = \left[\frac{\partial f}{\partial y_{P0}}(\mathbf{q}^\star)\right]^{-1} \left(\frac{\partial f}{\partial \kappa_O}(\mathbf{q}^\star)\Delta \kappa_O + \frac{\partial f}{\partial \kappa_A}(\mathbf{q}^\star)\Delta \kappa_A\right) \tag{29}$$

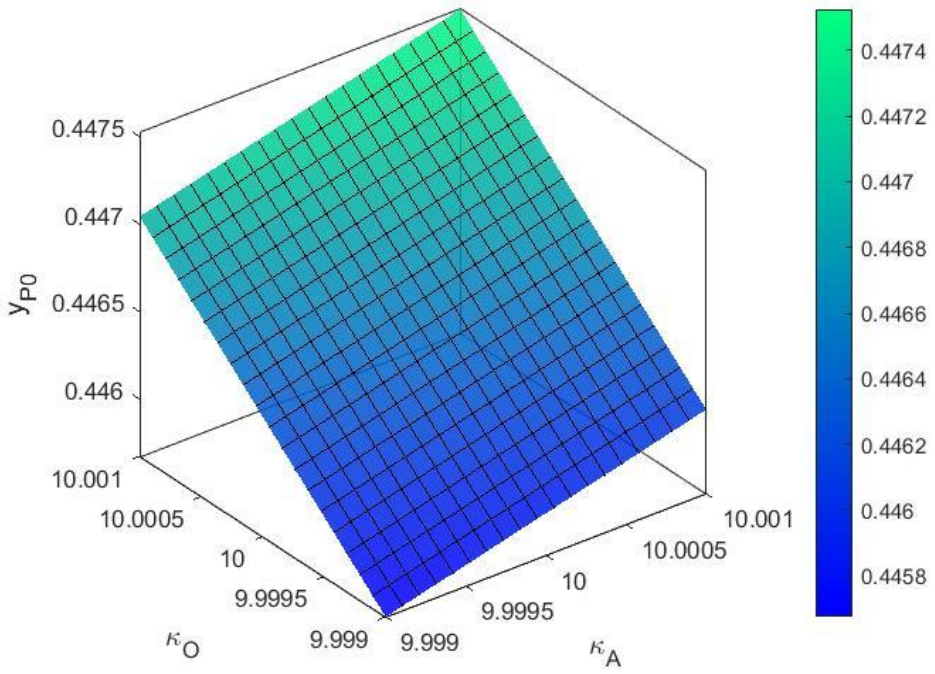

Figure 4. Portion of goal equivalent manifold (GEM) in 3D task variable space. The task variables represented by the $\boldsymbol{\kappa_O, \kappa_A, and\ y_{P0}\ axes}$, representing the torsional spring stiffnesses at joints *O* and *A*, and the initial puck location, respectively. The center point of this manifold is identical to $\mathbf{q}^\star$, the original parameter vector containing task variables corresponding to a successful target hit. All parameter points contained in the GEM also correspond to shots that hit the target.

As mentioned previously, all points that lie on this plane will give a goal equivalent error equal to zero. This also means fluctuations in task variables that are tangent to GEM result in errors that are goal equivalent, i.e., that to leading order have no effect on goal level error. Therefore, as you move further and further away from the GEM, the goal-error increases. In other words, the normal direction to the GEM will result in the greatest variability at the goal. The GEM provides a geometric sensitivity analysis that allows us to map body variability to the variability at the target.

4.2: Simulations with Fluctuations in Stiffnesses and Initial Puck Position

For a skilled player playing air hockey, the expectation is that each trial will a value $\mathbf{q} = (\kappa_O, \kappa_A, y_{P0})$ such that the error at the target is small i.e., a $\mathbf{q}$ that lies close to, but not on, the GEM. So, to simulate trials of a human playing air hockey, a random value for each of the parameters in the 3D task variable space was chosen. This value random value will be added to each of the values that make up $\mathbf{q}^\star$, respectively. Mathematically, this is represented by: $\mathbf{q} = \mathbf{q}^\star + \sigma\mathbf{q}$; where, σ is the noise strength or how large the deviation from $\mathbf{q}^\star$ is. An important item to note is that the GEM was defined without any consideration of the control that might be applied to correct errors from trial to trial.

For each trial, each task variable in the 3D space will be randomly assigned a gaussian normally distributed random number and the noise strength for each task variable will be held at a constant $\sigma = 10^{-4}$. The following data is for N = 1000 shots for a randomly generated task variable value. The plot on the left in **Figure 5** shows each one of the 1000 shots plotted in GEM task space. The distribution on the right in **Figure 5** shows the goal-error at the target. Also notice that for the distribution on the right, the center corresponds to $y = f(\mathbf{q}^\star) \cong 6.99672$.

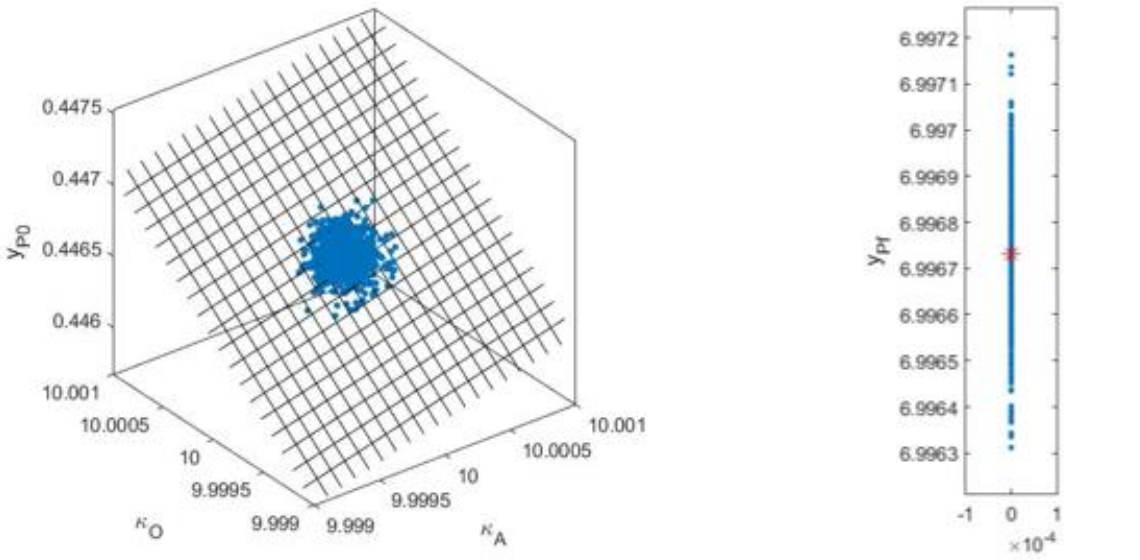

Figure 5. Shots on target for normally distributed random values of task variables. (left) Scatter plot of $N = 1000$ parameter points, each corresponding to a different shot on target. The random distribution of the shots represents physiological noise in human task performance; they are assumed to have a mean equal to $\mathbf{q}^\star$, as one expects for skilled task execution. (right) Variability at the target for every shot. The red star at the center of the scatter plot is the mean value of the shots and is also $\boldsymbol{f}(\mathbf{q}^\star) \cong \mathbf{6.99672}$ (see Eq. 23).

Figure 5 illustrates how body variability is mapped to goal level variability. This is because of the GEM. The GEM represents the geometric sensitivity of the task variables and demonstrates how fluctuations in each of the task variables is evident at the target.

Furthermore, since the probability distribution of the random parameters was gaussian and the noise strength was small, the distribution at the target should also be gaussian. These distributions are shown in **Figure 6**. The distributions indicate that body variability does relate to variability at the target. This is important for any type of goal directed motion, such as air hockey, because slight changes in the task variables effect the error of the output.

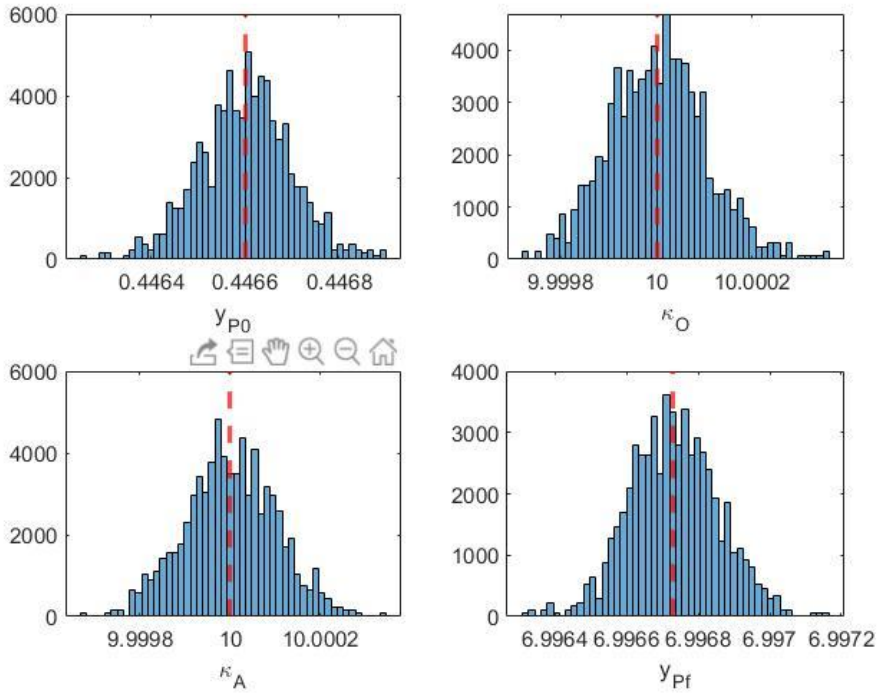

Figure 6. Empirical probability density functions (PDFs) for each task variable at target: (top let) puck starting position, y_{P0}; (top-right) torsional spring constant at shoulder hinge, κ_O; (bottom left) torsional spring constant at elbow joint, κ_A; (bottom right) the stopping position of puck after launch, y_{Pf}. The red dashed line in each figure represents the mean value of each distribution and corresponds to variable's value in $\mathbf{q}^\star$. The PDFs were estimated from the simulation data from N = 1000 shots (see Fig. 5).

The histograms above all show resemblance of a normal gaussian distribution. Also, the mean values for these distributions correspond to values given in $\mathbf{q}^\star$, respectively. Therefore, there exists a relation between the impedance task variables and the goal level error at the target. This allows for the examination of how each of the impedance task variables affects the goal of having the puck stop on the target. As evident in the histograms, the further from the mean value the randomly generated value is, the greater error at target. This is the equivalent of moving the value for a parameter in a direction that does not coincide with the tangent plane for the GEM.

Chapter 5

Conclusions and Future Work

The understanding of how humans are able to perform accurate and repeatable goal-directed movements has been a major goal of neuroscience research [1, 3]. While people have long known that the brain is divided into left and right hemispheres that each primarily control the contralateral side of the body, the motor regulation schemes implemented by each hemisphere is not yet understood. There exists a model for how brain lateralization is implemented known as the dynamic dominance model (DDM), which states that the left hemisphere (in right handers) implements a motion control scheme that successfully predicts the effects of the body and environmental dynamics, while the right hemisphere is proficient at impedance control processes to minimize the effect of unexpected disturbances [1]. The goal of this research was to develop a mathematical model of a human arm playing air hockey so that different actuation methods of the arm can be examined. The actuation method discussed in this research was based off an impedance system that contains springs and dampers.

The work presented in this thesis involved the design of a two-link mechanism that mimics a human arm playing air hockey. This involved deriving the equations of motion for both the mechanism and the puck after it is struck by the mechanism. The EOMs for the system include applied moments at the shoulder and elbow joints. These applied moments are arbitrary and can be varied depending on the motor control scheme being examined. For the impedance system, the applied moments were torsional springs that had effective stiffnesses and damping elements. The equilibrium positions of these EOMs were used to obtain an arm motion that struck the puck such that the puck travels along the y-axis. The EOM for the puck was determined by applying elementary collision dynamics and Newton's second law. The EOMs for the two-link

mechanism and puck result in function in which the inputs are system parameters (see **Table 2**) and its output is the final puck position. This is the goal function.

The goal function was used to compute the error for the target point on the y-axis. The linearization of the error was used to construct the tangent plane to the GEM around 3 system parameters that result in zero error, meaning these system parameters stop on the target. The parameters that were focused on were the torsional spring stiffnesses and the initial puck placement. These parameters were chosen because being able to analyze how changes in impedance elements is necessary for testing the dynamic dominance model. To examine these changes, 1000 shots on target were performed where each of the 3 parameters had a randomly assigned value that was close to t. The parameters for each shot plotted in the 3D task space with the GEM illustrated how body variability mapped to goal variability. The deviations in the 3D task space that are normal to the tangent plane result in a larger error at the target. This can also be seen by examining the empirical probability density functions in **Figure 6**. These distributions show that the greater variability from the value that results in zero error, the greater variability there is at the target.

The model for the air hockey game used in this research restricts the puck to only travel along the y-axis. However, a person playing air hockey does not always strike the puck with the intention of having the puck travel in a straight line. So, the target point needs to be expanded to any point in plane and not restricted to the y-axis. For this to be possible, a more general model of the collision between the mallet and the puck will need to be determined. In order to test the dynamic dominance model, a controller that updates the impedance variables between each shot also needs to be implemented. This can be done by examining the goal error the previous set of parameters produced and updating those as necessary. The impedance control scheme that will be implemented in the future is what will be used to test the impedance control scheme hypothesis present in the dynamic dominance model. The other element to the dynamic dominance model is

predictive control. To implement predictive control, the equations of motion need to adapt to represent a predictive system. This will involve replacing the applied moments at the shoulder and elbow joints with pre-defined torque time series or motor. The analysis of both the impedance model and the predictive model will aid in testing the dynamic dominance model.

Appendix A

MATLAB Code that Contains EOMs

```
function  [t,THETA] = odesrun(ti,tf,n_step,IC,options,p)
%{
This is a function that solves the EOM for my thesis mechanism.

INPUTS:
ti = intial time
tf = final time
n_step = step size of output
IC = row vector of inital conditions: [theta1_0 Dtheta1_0 theta2_0
Dtheta2_0]
p = is a parameter vector that contains:
    L = length
    m = mass
    theta1_un = unstretched spring length for point O
    theta2_un = unstretched spring length for point A
    kapA = stiffness MA
    cA = damping MA
    kapO = stiffness MO
    cO = damping MO
    xP = x-coordintate of puck
    yP = y-coordinate of puck
    tol = tolerance for event handler

OUTPUTS:
t = time array of soltuion
THETA = column vector containing sols for ODEs:
    theta1 = THETA(:,1)
    Dtheta1 = THETA(:,2)
    theta2 = THETA(:,3)
    Dtheta2 = THETA(:,4)
%}

% Call to Solver
[t,THETA] = ode45(@system,linspace(ti,tf,n_step),IC,options,p);
end

% function containing ODEs
function xdot = system(t,x,p)
%}
% extract paramters
L = p(1);
m = p(2);
theta1_un = p(3);
theta2_un = p(4);
kapA = p(5);
cA = p(6);
```

```
kapO = p(7);
cO = p(8);

% Convert to system of first order ODEs
denom = ((L^2)*m*(-23 + 9*cos(2*(x(1)-x(3))))); % compute denominator
before

xdot(1) = x(2);
xdot(2) = (-3*(8*(kapA*(-theta2_un+x(3)-x(1)) + cA*(x(4)-x(2)))) +...
        (8*(kapO*(x(1)-theta1_un) + cO*(x(2)))) +...
        (12*(kapA*(-theta2_un+x(3)-x(1)) + cA*(x(4)-x(2)))*cos(x(1)-
x(3))) -...
        (3*(L^2)*m*sin(2*(x(1)-x(3)))*(x(2)^2)) -...
        (4*(L^2)*sin(x(1)-x(3))*(x(4)^2)))/denom;
xdot(3) = x(4);
xdot(4) = (96*(kapA*(-theta2_un+x(3)-x(1)) + cA*(x(4)-x(2))) +...
        (36*(kapA*(-theta2_un+x(3)-x(1)) + cA*(x(4)-x(2)))*cos(x(1)-
x(3))) +...
        (36*(kapO*(x(1)-theta1_un) + cO*(x(2)))*cos(x(1)-x(3))) -...
        (48*(L^2)*m*sin(x(1)-x(3))*(x(2)^2)) -...
        (9*(L^2)*m*sin(2*(x(1)-x(3)))*(x(4)^2)))/denom;

% Transpsoe to Column vector
xdot = xdot';
end
```

Appendix B

MATLAB Code for Goal Function

```
function yPf = PuckPosV2(q)
%{
This is a function that determines the distance the puck travels along
the
y-axis before it stops and the of point just prior to the impact.
%}

% INPUTS are system parameters
kapO = q(1); % spring stiffness for torstional spring at O
cO = q(2); % damping for torsional spring at O
kapA = q(3); % spring stiffness for torstional spring at A
cA = q(4); % damping for torsional spring at A
theta1_un = q(5); % Unstretched spring angle for torsional spring at O
theta2_un = q(6); % Unstretched spring angle for torsioanl spring at A
yp0 = q(7); % intial position of puck on y-axis (xp0 = 0)

% system parameters that remain constant
L = 1;
m = 1;
theta1_i = pi/2;
theta2_i = -pi/2;
Dtheta1_i = 0;
Dtheta2_i = 0;
IC = [theta1_i Dtheta1_i theta2_i Dtheta2_i];

% set ODE solver parameters
tf = 100;
n_steps = 1000*tf;
tol = 0.0001; % can be updated

% puck postion
xP = 0;
yP = yp0;
rP = sqrt(xP^2 + yP^2);

% Solve ODE system
options = odeset('Events',@two_link_eventV3,'AbsTol',1E-12,'RelTol',1E-
12);
[t,THETA] =
odesrun(0,tf,n_steps,IC,options,[L,m,theta1_un,theta2_un,kapA,cA,kapO,c
O,xP,yP,tol]);
theta1 = THETA(:,1);
theta2 = THETA(:,3);

% path of B
xB = L*(sin(theta1) + sin(theta2));
yB = L*(cos(theta1) + cos(theta2));
rB = horzcat(xB,yB);
```

```
% Find beta
[beta,index] = beta_findV2(xB,yB,rP);

% Update system parameters
theta1_i_new = theta1_i - beta;
theta2_i_new = theta2_i - beta;
IC_new = [theta1_i_new Dtheta1_i theta2_i_new Dtheta2_i];
theta1_un_new = theta1_un - beta;

% Sovle ODE system again
options_new = odeset('Events',@two_link_eventV3,'AbsTol',1E-
12,'RelTol',1E-12);
[t_new,THETA_new] =
odesrun(0,tf,n_steps,IC_new,options_new,[L,m,theta1_un_new,theta2_un,ka
pA,cA,kapO,cO,xP,yP,tol]);

theta1_new = THETA_new(:,1);
theta2_new = THETA_new(:,3);
Dtheta1_new = THETA_new(:,2);
Dtheta2_new = THETA_new(:,4);

% New path of B
xB_new = L*(sin(theta1_new) + sin(theta2_new));
yB_new = L*(cos(theta1_new) + cos(theta2_new));
rB_new = horzcat(xB_new,yB_new);

% Velocity of B (with index for when beta is calculated)
vBx = L*((cos(theta1_new(index))*Dtheta1_new(index)) +
(cos(theta2_new(index))*Dtheta2_new(index)));
vBy = -L*((sin(theta1_new(index))*Dtheta1_new(index)) +
(sin(theta2_new(index))*Dtheta2_new(index)));

% Impact
e = 0.8; % COR
mu_k = 0.2; % kinetic friction

[tp,yPf] = impactV2(yp0,vBx,vBy,e,mu_k,n_steps);

yPf = yPf(end);
end
```

Appendix C

MATLAB Code for GEM, and Random Values

```
%%  GEM
% q_star
kapO = 10;
cO = 5;
kapA = 10;
cA = 5;
theta1_un = 0.7227;
theta2_un = -0.7227 - theta1_un;
yP0 = 0.4466;
q_star = [kapO cO kapA cA theta1_un theta2_un yP0];

% find gradient
h = 1e-6;
grad = center_diffV2(q_star,h);
pkO = grad(1); % partial derivatives for plotting
pkA = grad(3);
pyP0 = grad(7);

% GEM plot
delta = linspace(-1e-3,1e-3,20);
[delta_kO,delta_kA] = meshgrid(delta,delta);

delta_yP0 = (pyP0^-1)*(pkO*delta_kO + pkA*delta_kA);

%% Noise
% number of shots
N = 1000;

% noise stengths
sigmaO = 1e-4;
sigmaA = 1e-4;
sigmaP0 = 1e-4;

% preallocate
yPf = zeros(N,1);
kO_n = zeros(N,1);
kA_n = zeros(N,1);
yP0_n = zeros(N,1);

q_ran = rand(N,3);
% interate for shots
for i=1:N
    % random q vector
    q_noise  = [kapO+sigmaO*q_ran(i,1), cO, kapA+sigmaA*q_ran(i,2), cA,
theta1_un, theta2_un, yP0+sigmaP0*q_ran(i,3)]';

    % find final position
    yPf(i) = PuckPosV2(q_noise);
```

```
    % save q_noise kO,kA,yP0
    kO_n(i) = q_noise(1);
    kA_n(i) = q_noise(3);
    yP0_n(i) = q_noise(7);
end

%% Plotting
% read in GEM data
GEM_data = readmatrix('GEM_data_OK.txt');
delta_kO = GEM_data(:,1:20);
delta_kA = GEM_data(:,21:40);
delta_yP0 = GEM_data(:,41:60);

% read in random shot data
r_shot_data = readmatrix('r_shot_data_OK.txt');
kO_n = r_shot_data(:,1);
kA_n = r_shot_data(:,2);
yP0_n = r_shot_data(:,3);
yPf_n = r_shot_data(:,4);

% plot gem with random shots and q_star
kapO = 10;
cO = 5;
kapA = 10;
cA = 5;
theta1_un = 0.7227;
theta2_un = -0.7227 - theta1_un;
yP0 = 0.4466;
q_star  = [kapO cO kapA cA theta1_un theta2_un yP0]';

figure('name','GEM Plot with SHots')
%subplot(1,2,1)
plot3(kO_n,kA_n,yP0_n,'.','markersize',10)
hold on
plot3(q_star(1),q_star(3),q_star(7),'*','markersize',10,'markeredgecolo
r','r','linewidth',2)
surf(delta_kO,delta_kA,delta_yP0,'facecolor','none')
alpha 0.5
box on
axis equal
xlabel('\kappa_A','fontsize',12)
ylabel('\kappa_O','fontsize',12)
zlabel('y_P_0','fontsize',12)
hold off

figure('name','distributions')
%subplot(1,2,2)
xx = zeros(length(yP0_n),1);
plot(xx,yPf_n,'.','markersize',9)
hold on
plot(0,mean(yPf_n),'*','markersize',9,'markeredgecolor','r')
%plot(0,7,'*','markersize',9,'linewidth',2)
ylabel('y_P_f','fontsize',12)
axis equal
xlim([-1e-4 1e-4])
```

```
ylim([min(yPf_n)-1e-4 max(yPf_n)+1e-4])
%xlim([-0.001 0.001])

figure('name','histograms')
subplot(2,2,1)
histogram(yP0_n,50,'normalization','pdf')
hold on
xline(yP0,'--','linewidth',2,'color','r')
xlabel('y_P_0')

subplot(2,2,2)
histogram(kO_n,50,'normalization','pdf')
hold on
xline(kapO,'--','linewidth',2,'color','r')
xlabel('\kappa_O')

subplot(2,2,3)
histogram(kA_n,50,'normalization','pdf')
hold on
xline(kapA,'--','linewidth',2,'color','r')
xlabel('\kappa_A')

subplot(2,2,4)
histogram(yPf_n,50,'normalization','pdf')
hold on
xline(PuckPosV2(q_star),'--','linewidth',2,'color','r') % yPf from
q_star
xlabel('y_P_f')
hold off

% just GEM
figure('name','GEM')
surf(delta_kO,delta_kA,delta_yP0)
colormap winter
colorbar
alpha 0.85
axis equal
grid off
box on
xlabel('\kappa_A','fontsize',12)
ylabel('\kappa_O','fontsize',12)
zlabel('y_P_0','fontsize',12)
```

BIBLIOGRAPHY

[1] Sainburg, RL (2014) Convergent models of handedness and brain lateralization. frontiers in Psychology

[2] Yadav V, Sainburg RL (2014) Limb Dominance Results from Asymmetries in Predictive and Impedance Control Mechanisms. PLoS ONE 9(4): e93892. doi:10.1371/journal.pone.0093892

[3] John J, Dingwell JB, Cusumano JP (2016) Error Correction and the Structure of Inter-Trial Fluctuations in a Redundant Movement Task. PLoS Comput Biol 12(9): e1005118. doi:10.1371/journal. pcbi.1005118

[4] Mutha PK, Haaland KY, Sainburg RL (2013) Rethinking Motor Lateralization: Specialized but Complementary Mechanisms for Motor Control of Each Arm. PLoS ONE 8(3): e58582. doi:10.1371/journal.pone.0058582

[5] Cusumano, J.P., Cesari, P. Body-goal Variability Mapping in an Aiming Task. *Biol Cybern* **94,** 367–379 (2006). https://doi.org/10.1007/s00422-006-0052-1

[6] Cusumano JP, Dingwell JB (2013) Movement variability near goal equivalent manifolds: Fluctuations, control, and model-based analysis. ScienceDirect. https://doi.org/10.1016/j.humov.2013.07.019

[7] Cusumano JP (2018) Notes on 2D Shuffleboard With Impulsive Launch: Goal Function, GEM, and Sensitivity at the Task Level.

Zachary Morgen

Education

The Pennsylvania State University, State College, PA
- Bachelor of Science: Engineering Science and Mechanics
- Minor: Engineering Mechanics
- Schreyer Honors Scholar
- Graduation Date: May 2022

Perryville High School, Perryville, Maryland

Work Experience

Academic Peer Tutor, Penn State Brandywine, Media, PA Sept 2019 - Present
- Tutor students in such areas as Math, Physics, and Chemistry delivering one-on-one and group tutoring sessions.
- Assisting students in the understanding and clarification of challenging concepts.
- Helped each student build strong study habits and use effective learning strategies.

Orientation Leader, Penn State Brandywine, Media, PA Summer 2019
- Guided campus tours with as many as 20 students and families.
- Supported registration processes with technical assistance and troubleshooting.
- Mentored students and families on successful strategies for college life.
- Planned and led activities and events to promote bonding among incoming students.
- Received Orientation Leader of the Year Award.

Design Projects

Design Team Leader for Redesign of Electric Toothbrush Fall 2018
- Supervised team of Engineering undergraduates.
- Ensured that team was meeting deadlines through effective communication.
- Used CAD software to create prototypes.

International Design Team Leader for Design of Shopping Cart Fall 2018
- Supervised team of Engineering undergraduates.
- Collaborated with students from South America.
- Ensured that team was meeting deadlines through effective communication.
- Used CAD software (SolidWorks) and 3D printing technology to produce prototypes.
- Responsible for the presentation of team's final design.

Computer Skills

Extensive Working Knowledge of Microsoft Word, Excel, PowerPoint, MATLAB, SolidWorks, AutoCad, Fusion 360, Working Model

Honors/Activities

Dean's List (Fall 2018, Spring & Fall 2019, Spring & Fall 2020, Fall 2021), Secretary of Chess Club (2019-2020), Vice President of Math Club (2018 - 2020), Society of Engineering Science Member (2020 – 2022)